AIMS Molecular Science

AIMS Molecular Science, 11(4): 395–414.
DOI: 10.3934/molsci.2024024
Received: 28 July 2024
Revised: 16 November 2024
Accepted: 25 November 2024
Published: 18 December 2024

http://www.aimspress.com/journal/Molecular

Research article

Investigation of biocorrosion on mild steel in cooling tower water and its inhibition by *C. sativum*

Sharmil Suganya R*, Stanelybritto Maria Arul Francis and Venugopal T

Government College of Engineering, Salem-11, Tamil Nadu, India

*** Correspondence:** Email: sweetsharmil@gmail.com.

Abstract: The primary goal of this investigation was to evaluate the effect of *Coriandrum sativum* extract on mitigating corrosion caused *by Staphylococcus aureus*, *Klebsiella pneumonia*, and *Bacillus subtilis* on metal samples. Analytical methods including SEM, FTIR, and XRD examination were used on the metal surface to determine the mechanism underlying corrosion inhibition. Impedance studies and Nyquist plots were used to support the role of green inhibitors in biocorrosion control. Based on analytical examinations, the corrosion patterns in some pitted zones showed a substantial link between microbial metabolites and the chemical composition of the metal surface. The presence of microbial metabolites caused the metallic surface to become more porous and permeable, changing the surface's structural makeup. In all three bacteria, 30 ppm of plant extract was found to be the maximum concentration that inhibited microbial corrosion. The coupons submerged in the control solution lost weight, indicating that the addition of the inhibitor caused a brief increase in corrosion rates before they declined.

Keywords: microbial-induced corrosion; biofilm; plant extracts; Nyquist plots; SEM; FTIR

1. Introduction

Microorganisms cause an increase in corrosion through an electrochemical process known as biocorrosion, microbiologically influenced corrosion (MIC), or microbial corrosion. Because of their interactions with the surroundings of the metal surface, microorganisms present in the environment can induce a variety of consequences. Given the strength of this interaction, it is reasonable to assume that the microbial involvement in corrosion will be evident in increased metal damage.

Weight loss studies and electrochemical methods are primarily used to determine corrosion inhibition; however, the mechanistic elements of plant-mediated biocorrosion inhibition have received less attention. There is very little evidence available about plants' potential to suppress microbial corrosion, but there has been a recent increase in the number of researchers engaged in this field. Therefore, a thorough analysis of the microorganisms that cause corrosion as well as the mechanism by which plant extracts block corrosion has been conducted. The chemical composition of the mild steel under study was found to consist of Fe, Mn, Si, Cu, Cr, C, Ni, W, Al, Mo, V, and Co at weights of 96.7%, 0.45%, 0.27%, 0.12%, 0.10%, 0.12%, 0.11%, 0.05%, 0.02%, and 0.03%, respectively.

According to the results in [1], *S. aureus*, *B. subtilis*, and *K. pneumoniae* present moderate bacterial activity and a good ability to mild steel corrosion in 1M H_2SO_4. When tested with various human pathogenic bacteria, including *E. coli*, *B. subtilis*, *S. typhimurium*, K. *pneumoniae*, *S. aureus*, and *P. aeruginosa*, *C. albicans* displayed distinct inhibitory zones of varying sizes [2].

The herbal plant *Coriandrum sativum* (taxonomic profile: Kingdom, Plantae; Subkingdom, Tracheobionta; Division, Magnoliophyta; Superdivision, Spermatophyta; Class, Magnoliopsida; Subclass, Rosidae; Order, Apiales; Family, Apiaceae; Genus: *Coriandrum* L.; Species: *Coriandrum sativum* L is well-known for its therapeutic applications [3]. One of the most frequently documented biological properties of its leaves is their anti-microbial activity [4–6]. According to [3], they demonstrated inhibitory action against both gram-positive and gram-negative bacteria, including *S. aureus*, *Bacillus spp*., *E. coli*, *P. aeruginosa*, *S. typhi*, *K. pneumoniae*, and *P. mirabilis*. According to [7], *C. sativum*'s phytochemical screening revealed the presence of flavonoids, phenolics, tannins, terpenoids, reducing sugars, essential oils, fatty acids, sterols, and glycosides [8,9].

Cooling towers are essential for maintaining consistent machinery temperatures and releasing heat while a machine is operating. Numerous factors, including the concentration of dissolved inorganic salts, ambient temperature, pH, moisture content, and microbial activity, all work together to promote the progression of corrosion in these systems. As stress concentrators, corroded areas can lead to component failure, systemic instability, and eventually catastrophic collapse. Cooling towers are also susceptible to malfunction over time due to harsh operating environments and conditions, which commonly results in general issues [10].

The term “microbiologically influenced corrosion” (MIC) refers to the theory used to explain how microbes affect the rate at which corrosion processes on both metal and non-metallic surfaces progress. Microbes have a major impact on corrosion, particularly on metal surfaces. Numerous bacterial populations produce secretions and form biofilms. These films are formed when bacteria grow on metal surfaces, forming different microenvironments that change the hard, solid surface's wettability and electrostatic charge, facilitating the colonization of bacteria in the outermost layer. Surface damage and an acceleration of corrosion rates are caused by this mechanism [11].

Localized corrosion results from the corrosion that starts and grows beneath this biofilm. Over an unmonitored period of exposure, this localized corrosion causes metal wall holes to grow [12]. A paradigm change away from dangerous corrosion inhibitors and toward more affordable, non-toxic, and biodegradable options is required due to rapid industrialization [13]. In recent years, plant extracts have become increasingly popular as safer substitutes for these organic and inorganic inhibitors [14].

Plant extracts have the ability to prevent corrosion on metal surfaces. Organic phytochemicals that exhibit antibacterial activities against a range of microbes, such terpenoids and other

hydrocarbons, are more likely to be adsorbed on a metal surface. The use of plant extracts as green corrosion inhibitors is undergoing a paradigm change, and this has shown to be a promising area of study [15].

To assess how microorganisms affect corrosion arising from their interactions with a metallic surface, three specific bacteria have been chosen*: Staphylococcus aureus*, *Klebsiella pneumonia*, *and Bacillus subtilis*. Studies were conducted to look at how extracts from *Coriandrum sativum* affected biocorrosion. The creation of environmentally friendly materials is crucial to lowering the number of bacteria that live on metallic surfaces. Ecologically friendly formulations are advised to reduce negative effects on the environment and stop corrosion on the metallic surface. In order to understand how plant extracts control microbial corrosion, a multimodal approach that integrates metal surface contacts and microbial chemistry was used to obtain high inhibitory efficiency.

2. Materials and methods

2.1. Collection of cooling tower water (CTW) and processing of steel coupons

Fine chemicals of analytical reagent grade were purchased from Himedia for use in microbiological experiments. The cooling tower water from the Mettur thermal power station was collected for laboratory use in autoclave-sterilized bottles and placed in an ice box. Average pH was within 7.8–8.3. Between 138 and 200 mg/L of TDS were present. The water in the cooling tower was between 27 and 30 °C. After being cleaned with ethanol and polished to a final surface finish, the mild steel coupons were allowed to air dry in a desiccator. Both before and after the experimental research, the dry coupons were weighed. The dirt was cleaned from mild steel coupons of 6 cm × 1 cm using a pickling process, and weight loss measurements were made. Mild steel coupons of 1 cm × 1 cm were used for polarization and impedance analysis; these were not cleaned with a pickling solution or water.

2.2. Microbial culture and preparation

Three bacterial strains—*Staphylococcus aureus*, *Bacillus subtilis*, *and Klebsiella pneumonia*—were chosen and subcultured in Luria Bertani (LB) broth in accordance with standard recommendations [16]. One milliliter of the microbial culture with a cell density of 107 CFU/mL was seeded into 100 mL of sterile LB broth and incubated in the shaker incubator for 50 min. After that, bacterial strains were kept in a temperature-controlled incubator at 37 ℃.

2.3. Soxhlet extraction

Coriandrum sativum seeds were obtained from the nearby marketplace. Extraction was performed from seeds ground into a fine powder and sieved. A thimble containing 10 g of the powdered material was put inside the Soxhlet extractor. The 10 g powdered sample was mixed with 200 mL of ethanol, and the oil was extracted for 48 h, keeping the solute/solvent ratio at 1:10. Refluxing temperature was 55 ℃. Any leftover ethanol was eliminated using a rotary evaporator, resulting in essential oils.

2.4. Well diffusion method

The well diffusion test was carried out in compliance with accepted practices [17]. Using a sterile L rod, 100 µL of the bacterial suspension was transferred into the appropriate Petri plate with solidified LB agar. Using a sterile cork borer (7.5mm), 7 mm diameter wells were created in the agar medium. Three distinct concentrations of green inhibitors (10, 30, and 50 µL) were then added to each well. Amoxicillin and dimethyl sulfoxide (DMSO) served as the controls. After a 24h incubation period, the minimum inhibitory concentration (MIC) of each plate was determined by measuring the zones of inhibition with digital vernier calipers.

2.5. Weight loss method

A conventional procedure was followed for the weight reduction study, with a few minor adjustments [18]. The microbial system, consisting of the corrosion inhibitor reaction mixture, contained 1 mL of each of the three microbial cultures devoid of mild steel coupons, 400 mL of sterile cooling tower water (CTW), and nutritional broth (1% w/v). The control was a sterile polished mild steel coupon that was submerged in 400 mL of sterile cooling tower water. Then, in a sterile inoculation chamber, coupons made of polished, sterile mild steel were submerged in the sterile media. Then, 10, 20, 30, and 50 µL of various plant extract concentrations were applied to the corresponding flasks. The mild steel coupons were collected, allowed to air dry, and then weighed to determine how much weight had been lost as a result of the corrosion process.

2.6. Corrosion analysis

For each system, a triplicate analysis of the corrosion rate was performed. The coupons were taken out of the conical flasks, autoclaved, and weighed once a week. The coupons were submerged in the pickling solution [1000 mL of 0.1 N hydrochloric acid containing 20g (w/v) of antimony trioxide and 50 g (w/v) of stannous chloride] for 25 min at room temperature in order to conduct studies on weight loss assessment. The corroded coupons that had been treated with acid underwent XRD and SEM investigation. Three weeks later, the coupons were taken out of their systems, and each metal's corrosion products were scraped off and examined [18].

2.7. Electrochemical studies

An electrochemical workstation (Model CH 1608 D/E Series) with a platinum electrode and a reference electrode (a saturated calomel with Ag/AgCl) was used for electrochemical investigations. Using a three-electrode cell, mild steel coupons (1.0 × 1.0 cm^2) were employed for electrochemical research [18].

2.8. X-ray diffraction (XRD) spectroscopic analysis

An X-ray diffraction device (Wilcox 132 XRD analyzer) with a maximum power of 12 KW (60 kV and 200 mA) was used to evaluate metal scraped from mild steel [19].

2.9. Scanning electron microscopy (SEM)

The corrosion products underwent a process of scraping, crushing, and coating with Au/Pd using a Bio-Rad Polaran E5400 high-resolution sputter coater. They were then mounted on aluminum holder stubs using double sticky carbon tape. At 15 KV, they were inspected under a ZEISS scanning microscope (Elvis 15, Germany). To find microstructural differences, the SEM images were analyzed [20].

2.10. Fourier transform-infrared (FTIR) analysis

The Perkin Elmer model was used to obtain the oil sample's Fourier transform-infrared spectra. At a resolution of 4 cm^{-1}, the absorbance was measured in the wavelength range of 4000 cm^{-1} to 400 cm^{-1}. KBR was utilized to pellet the materials, and the pellets were then employed for additional analysis [21].

2.11. Gas chromatography–mass spectrometric (GC–MS) analysis

Using Bruker 45X (GC) and SC-ION (MS) equipment with a mass detector, GC–MS analysis was carried out in a linked workstation. The capillary column (15 m in length) was filled with helium carrier gas at 70 ℃ with a 5-min holding period. A 45 min total run duration was maintained by injecting 1 µL of the sample at a flow rate of 1 mL/min into the GC column. The metabolites were identified by comparing the GC–MS peaks with the National Institute of Standards and Technology (NIST) database after the separated metabolite mass spectra (70 eV) were recorded. According to [22], the ethanol extract's GC–MS peaks revealed the existence of bioactive chemicals.

3. Results and discussion

Corrosion on the metallic surface may be harmful due to the existence of microbiological consortia, which are groups of different microbe species living together within a biofilm [23]. The process of biocorrosion is aided by a wide range of microorganisms, such as those that reduce sulfates and metal, oxide metal, are acidic and slime-forming, consume and produce hydrogen, and are both aerobic and anaerobic [24]. Because of the activation of numerous biochemical processes at the oxic–anoxic transition zone, multiple species coexist and contribute to the corrosion process, which has a detrimental and direct impact on both human health and commercial activities [25].

3.1. Anti-microbial studies

The well diffusion method was the main testing strategy employed in the current study to ascertain whether the three chosen plant extracts might inhibit microorganisms under in vitro study. The zones of inhibition caused by essential oils are shown in Table 1. *Coriandrum sativum* was employed at three concentrations (10, 30, and 50 µL for T1, T2, and T3, respectively). As negative and positive controls, 50 µL of DMSO and sterile amoxicillin discs were utilized. According to previous studies, phytoconstituents found in *Coriandrum sativum* have antibacterial action and prevent the growth of biofilm [26]. Nonetheless, there was no discernible difference between the

three concentrations (T1, T2, and T3). The plant extract at 30 ppm was reported to result in a higher inhibition zone. Figure 1 depicts the inhibition zones of *Coriandrum sativum*.

Essential oils have antibacterial properties because of their secondary metabolites, which interact with the lipids in the cell membranes of bacteria to cause metabolic disruption and cellular death. Bacteria release secondary metabolites, which are essential for both cellular growth and death. By altering the structure of cell membranes and the enzymatic machinery, these secondary metabolites stop bacteria from proliferating [27]. The cell membrane is essential to the integrity of cells as well as the transport of nutrients, energy, and information between the cells and their environment. When the bacterial cell membrane degrades, macromolecules like proteins and nucleic acids leak out [28]. This has the antibacterial effect of preventing microbial growth or cell death.

Table 1. Diameters of clear inhibition zone using the well diffusion method.

Plant extract	Microbes	Negative control (mm)	Positive control (mm)	T1 (10µL) (mm)	T2 (30µL) (mm)	T3 (50µL) (mm)
Coriandrum sativum	*S. aureus*	10	13	11	12	13
	B. subtilis	10	12	11	13	14
	K. pneumoniae	10	11	11	13	13

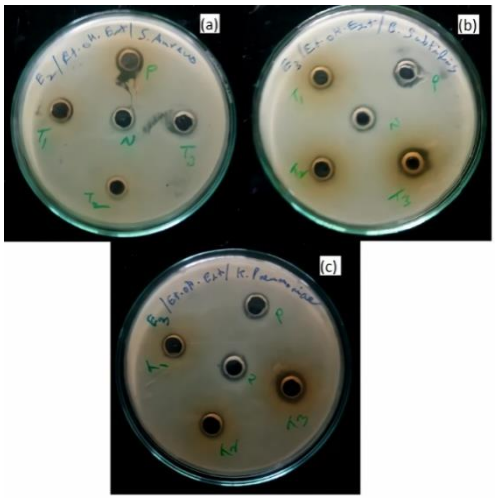

Figure 1. Inhibition zone of *Coriandrum sativum* on plates spread with (a) *S. aureus*, (b) *B. subtilis*, and (c) *K. pneumoniae*.

3.2. Surface analysis

The corrosion products were collected, ground into a fine powder, and used in Fourier-transform infrared spectroscopy (FTIR) and X-ray diffraction spectroscopy (XRD). Using a sterile spatula, the surface coating was scraped off and then dissolved in methanol for additional examination.

3.2.1. SEM analysis

SEM pictures of mild steel coupons subjected to cooling tower water contaminated with microbes show how biofilms grow and eventually corrode the material. Variations in cell concentrations promote bacterial adhesion to the steel surface, enabling the formation of biofilms that include exopolysaccharides (EPS) that serve as a diffusion barrier against corrosive agents. The corrosion process is accelerated by the cells that are located in areas with higher oxygen concentrations, variable biofilm thickness, and irregular distribution of EPS and other corrosion by-products. Due to chemical or electrochemical interactions between the exposed surface and the surrounding environment, the structural composition and properties change during the corrosion process [29].

There is an accumulation of corrosion particles on the metallic surface, giving the corrosion pattern a highly heterogeneous appearance. Furthermore, the presence of microorganisms suggests a high surface interaction, resulting in the creation of pits in certain areas and apparent scratches on the surface. The metal surface has a significant density of accumulation and fissures, according to SEM analysis.

According to research by [30], there are three steps in the process of microbe-induced corrosion initiation: the microbial consortium's physical adherence, the harboring and release of corrosive metabolites, and the depolarization of the metal surface at the surface of the hydrophobic substrate. Under biological conditions, increased corrosivity is caused by the growth and harboring of microbial consortia, which in turn produce and release corrosive metabolites into the surrounding environments. The structural elements of the material under investigation are changed by the released corrosion metabolites, which increases the porosity and permeability of additional corrosive materials into the pitted zone [31].

The *Coriandrum sativum*-treated mild steel is shown in Figure 2. Plant extracts, often known to be corrosion inhibitors, have a notable impact on the metal surface, impeding its disintegration. The three bacteria that cause corrosion—*S. aureus*, *B. subtilis*, and *K. pneumonia*—were found to be successfully suppressed by the plant extract. Figure 3 (a) depicts the SEM picture of the microbe-free control, and Figure 3(b)–(d) show the control SEM images of the three mild steel samples treated with microorganisms (B: *S. aureus*, C: *B. subtilis*, and D: *K. pneumoniae*) but not with plant extracts.

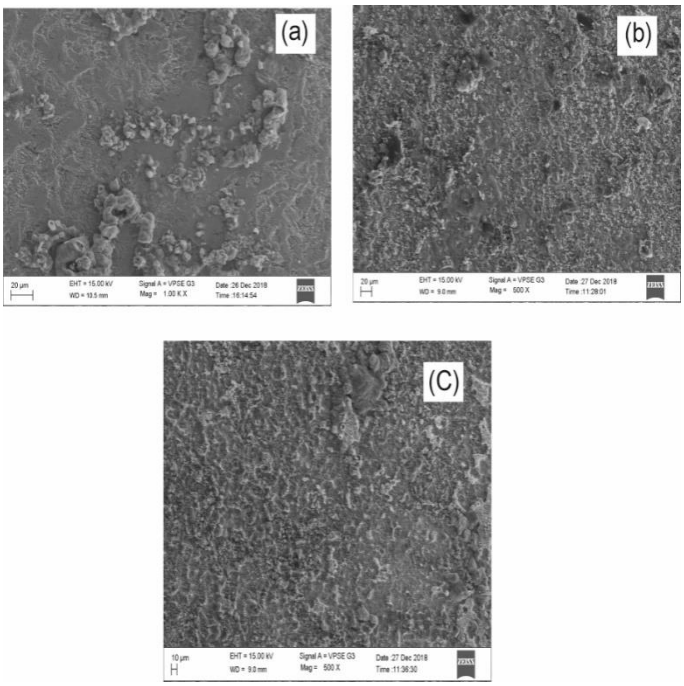

Figure 2. SEM analysis of *Coriandrum sativum*-treated surfaces of mild steel.

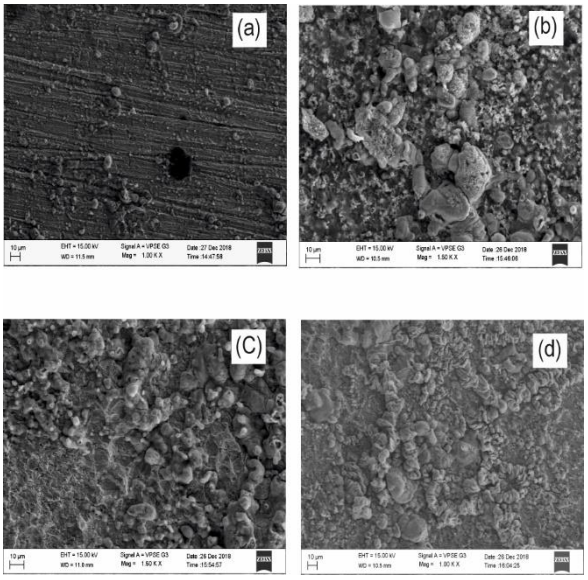

Figure 3. SEM analysis of control and microbe-coated mild steel structures.

3.2.2. FTIR

After being removed from the rusted mild steel surface, samples were examined using FTIR technology. Figure 4 represents the FTIR analysis of the corroded samples. The hydroxyl groups of water molecules that were attached to the surface are responsible for the peak that was seen at 3409 cm^{-1}. Peaks at 1631cm^{-1} could be related to the O-H stretching mode, surface hydroxyl, and bending vibration of absorbed water. Fe_2O_3/FeS is the most likely cause of the peaks at 518 cm^{-1} and 620 cm^{-1} [32].

Several bands below 600 cm^{-1} in the FTIR spectrum of *Coriandrum sativum* are associated with the functional groups of organic acids, flavonoids, and alkaloids. Many bacterial strains produce biofilms, and one important aspect of this process is the presence of bacterial plasmids.

The facilitation of contacts between polar and non-polar functional groups is significantly influenced by the hydrophobicity of the cell surface. Furthermore, a crucial step in the formation of biofilms is the microbe's motility across the metal contact surface [33].

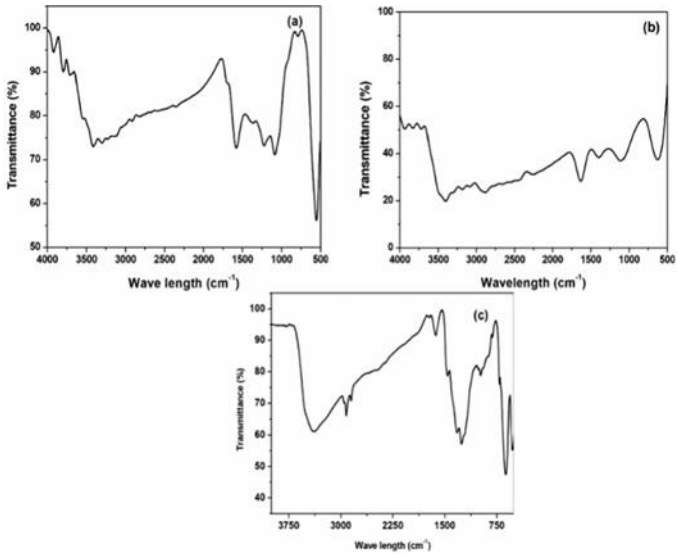

Figure 4. FTIR analysis of the corroded samples.

3.2.3. XRD analysis

After being scrapped, the mild steel surface was examined using XRD. XRD analysis evaluated the biocorrosion process caused by the three microorganisms (*S. aureus* (A), *B. subtilis* (B), and *K. pneumonia* (C)) (Figure5). Iron hydroxide (FeOOH) and ferrous sulfide (FeS) are represented by peaks in the XRD pattern of pure mild steel treated in cooling tower water (CTW) [34]. Surface deposits of corrosion products (FeS) are observed on mild steel that has undergone CTW treatment. When a biocorrosion inhibitor was added to mild steel that had been eroded by microbes, new peaks would occasionally vanish and reappear because the biofilm growth on the mild steel's exterior was inhibited. Peaks linked to iron oxides like Fe_3O_4 and FeOOH appear to be vanishing. This shows that the protective coating contains no trace of iron oxide and that the metal's surface is completely shielded against corrosion. According to [35], inhibitors such as carbon, nitrogen, oxygen, and phytochemicals can minimize iron peaks on metals and create a protective layer.

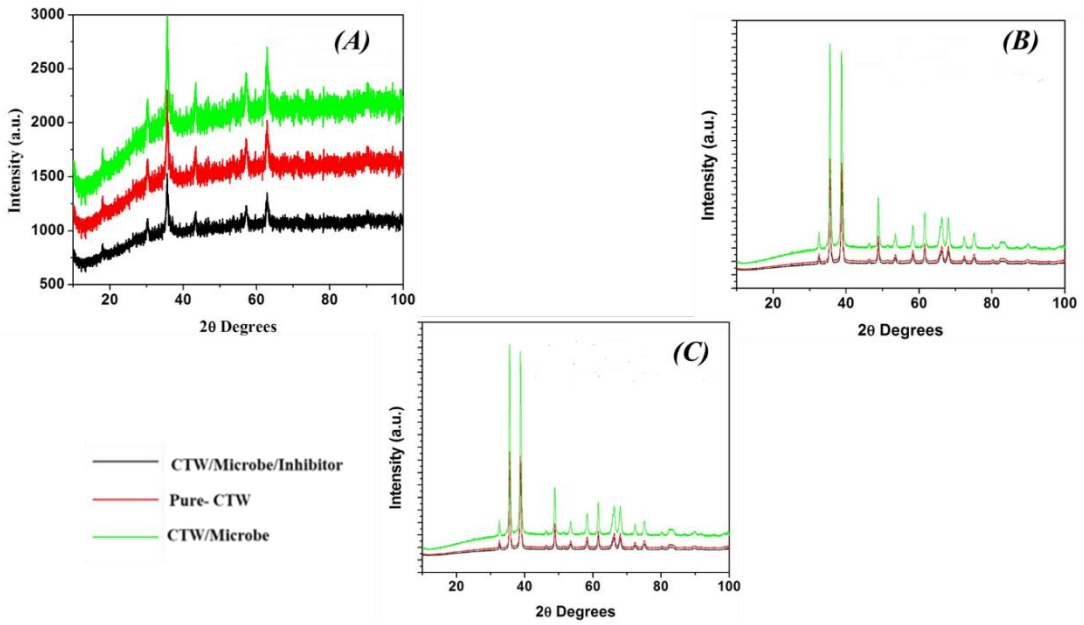

Figure 5. XRD analysis of the biocorrosion process.

3.3 GC–MS analysis

Figure 6 represents the GC–MS analysis of *Coriandrum sativum*, showing the presence of cyclopentanone, 2-methyl, (2-mercaptoethyl) guanidine, 1,2-diethylhydrazine, benzene, 1-methyl-3-(1-methylethyl), ç-terpinene, propane, 1,1,3-triethoxy, and linalool [36]. According to published research, secondary metabolites are essential for providing a protective layer on the surface and for the inhibitory effect on bacterial development [37].

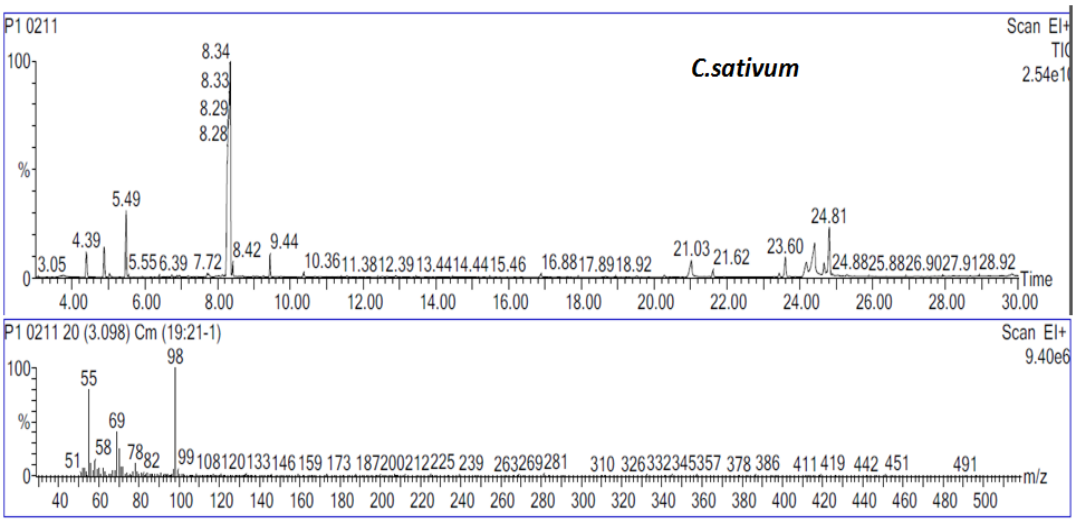

Figure 6. GC-MS analysis of *Coriandrum sativum*.

3.4. Electrochemical impedance

An investigation of electrochemical impedance was conducted in cooling tower water systems with and without microorganisms and inhibitors [38]. Further significant characteristics, such as charge transfer resistance (R_{ct}) and double-layer capacitance (C_{dl}), were calculated based on impedance spectrum analysis [15]. The impedance parameters obtained from Nyquist plots are shown in Table 2. There was a considerable variance in mild steel's susceptibility to different ecosystems [39]. The impedance of steel varied and showed a rising trend as the exposure period increased. This rise suggested that the pace at which steel corroded in sterile culture conditions was regulated, with variability most likely being determined by the corrosion product. At higher frequencies, the negative value of the phase angle may be the cause of the system disruption. A capacitive semicircle was detected at high frequencies, which may have been caused by biofilm formation and the deposition of corrosion products on the surface layer. Charge transfer mechanisms may play a role in the development of metallurgical dissolution, which could account for a minor capacitive loop found at low frequencies.

Table 2. Impedance parameters derived from Nyquist plots.

Immersion of MS in systems	R_s	R_{ct} (ohm cm^2)	C_{dl} (F/cm^2)	θ	IE (%)
S.aureus	211.7	4885.80	1.17×10^{-13}	0.7953	79.53
S.aureus and C. sativum	253.2	8299.40	9.10×10^{-14}	0.8795	87.95
B.subtilis	271.2	9476.00	6.94×10^{-14}	0.8945	89.45
B.subtilis and C. sativum	274.2	14396.20	6.78×10^{-14}	0.9305	93.05
K.pneumoniae	193.0	5218.00	9.11×10^{-14}	0.8084	80.84
K.pneumoniae and C. sativum	230.3	8069.80	7.35×10^{-14}	0.8761	87.61

Note: R_S: Solution resistance; R_{ct}: Charge transfer resistance: C_{dl}: Double layer capacitance.

Impedance characteristics such as solution resistance, charge transfer resistance, and double-layer capacitance values were derived from the Nyquist plots. By comparing the charge transfer resistance of inhibited and unrestrained cells, the inhibition efficiency was computed [40]. Nyquist plots showed that single semicircles acted as capacitive loops in the high-frequency band, signifying resistance to charge transfer both with and without an inhibitor (plant extracts). A linear link between the semicircle and biofilm load has been seen in earlier research, indicating that biofilm adhesion to the mild steel surface inhibits charge transfer and lowers the rate of corrosion [41].

Enzymes and metabolites produced by bacteria affect the interactions between solid materials and fluids in microbiological ecosystems. These byproducts have the ability to change the outermost layer's electrochemical properties, which can impact the rate of corrosion and the surface's propensity to absorb or release electrons [42]. Because biofilms release naturally occurring polymers, they are stable both physically and functionally. Complex biofilms on solid surfaces are formed in part by microorganisms in bio-electrochemical systems [43]. These microbes release metabolites, proteins, genetic materials, and exo-polysaccharides, which are encapsulated in extracellular polymeric compounds. These molecules are necessary for the production of biofilm deposits and are closely linked to the synthesis of extracellular polymers.

The Nyquist plot diameter and biofilm formation have a linear relationship. In Nyquist plots, a bigger semicircle width often denotes a stronger electrical resistance at the metal–solution interface, which suggests a lower rate of corrosion. Under comparable working circumstances, the *Coriandrum sativum* extract effectively reduced microbe-induced corrosion by preventing the formation of biofilms. According to reports, the bacteria that the extract inhibited were, in increasing order, *Bacillus subtilis*, *Klebsiella pneumoniae*, and *Staphylococcus aureus*. According to [26], phytoconstituents found in *Coriandrum sativum* demonstrated anti-microbial activity by preventing the growth of biofilm (Figure 7). The R_{ct} values indicate that plant inhibitors were confined to the outermost layer of mild steel, acting as a controlled protective barrier, retarding the rate of the corrosion process. Electrochemical impedance data revealed that plant extracts effectively mitigated the development of microbial biofilms over the metal surface. Based on R_{ct} data, it was concluded that *Staphylococcus aureus* + *Coriandrum sativum* reported low current consumption, followed by *Klebsiella pneumonia*, and finally *Bacillus subtilis* [5]. The green inhibitors act as an additional layer of protection, regulating and delaying the corrosion process on the outermost layer of mild steel specimens [44].

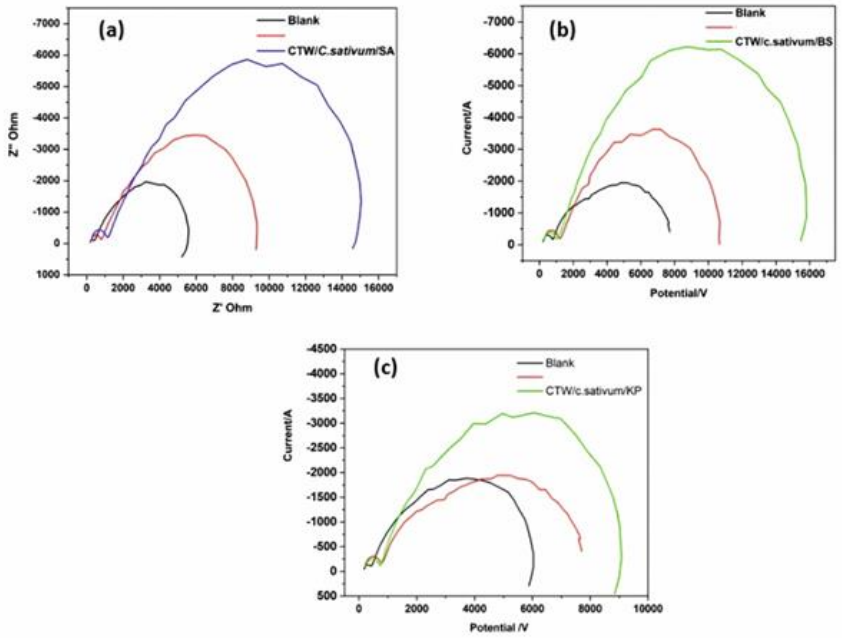

Figure 7. Impedance analysis of *Coriandrum sativum*.

Through the exchange of electrons, positively charged plant extract (inhibitor) molecules formed contacts (adsorption) with negatively charged metallic surfaces [45]. By lowering current consumption and corrosion rates as well as creating protective layers, these green inhibitors reduce microbial adherence on the metal surface [46]. Figure7 represents the impedance analysis of *Coriandrum sativum*.

Biofilm production is linked to the growth of microorganisms and the components they release, and this has a substantial effect on the surface double-layer capacitance (C_{dl}) of mild steel. The capacitance development of the research in all three areas of investigation ranged from 1.4×10^{-13} to 5.2×10^{-13}. The formation of biofilms and the decrease in double-layer capacitance are strongly

related. The production of metabolites during bacterial growth and the availability of nutrients are essential for the establishment of biofilms [47]. Most of the adsorption sites for mild steel are made up of bacteria and their components. As the biofilm grows, the double-layer capacitance becomes less sensitive, indicating that variables outside of the bacterial cell may affect the capacitance while it is being evaluated [48]. Technically, only a certain amount of charge can be stored in that restricted zone, and the properties of the electrolyte and the experimental design dictate how thick the double layer is [49]. In all three categories, experimental investigations showed that the plant extracts could block, on average, over 80% with more than 75% surface coverage.

3.5. Tafel plots

The formation of biofilms and the metabolic mechanisms of some bacterial strains promote microbial corrosion. Certain plant extracts have been found to possess antibacterial characteristics, which help to reduce biocorrosion [50]. Table 3 shows the polarization parameters for mild steel in the control, microbial (*S. aureus*, *B. subtilis*, and *K. pneumoniae*), and inhibitor (*Coriandrum sativum*) systems. According to published research, the rate of corrosion increases with increasing corrosion potential and vice versa [51]. The Tafel characteristics, including the cathodic and anodic Tafel slopes (β_a, β_c), corrosion potential (E_{corr}), and corrosion current density (I_{corr}), were obtained from the potentio dynamic polarization curves [15]. Only certain factors can determine if a chemical is anodic, cathodic, or mixed-type inhibitor based on its E_{corr} value [52]. The polarization curves in the presence of the *Coriandrum sativum* plant extract + microbial system + CTW shifted toward the more negative potentials compared to CTW and CTW + microbial system, indicating the more predominant cathodic inhibition activities of the plant extracts (*C. sativum*).

Table 3. Polarization parameters for mild steel in control, microbial (*S. aureus*, *B. subtilis*, *K. pneumoniae*), and inhibitor *(Coriandrum sativum)* systems.

Immersion of mild steel in systems	$-E_{corr}$ (V)	I_{corr} (A/cm^2)	R_p (Ω)	β_a (V/dec)	β_c (V/dec)	θ	IE (%)
Control	0.945	1.68×10^{-5}	5927	7.404	3.620	--	--
S.aureus	0.989	4.94×10^{-6}	7851	7.476	3.730	0.7055	70.55
S.aureus and*C. sativum*	0.975	3.0×10^{-6}	9417	9.341	3.174	0.8100	81.00
B.subtils	0.999	4.42×10^{-6}	8378	7.607	3.158	0.7310	73.10
B.subtilis and*C. sativum*	0.975	2.62×10^{-6}	13421	9.512	2.847	0.8438	84.38
K.pneumoniae	1.000	4.48×10^{-6}	6006	1.075	4.993	0.7332	73.32
K.pneumoniae and*C. sativum*	0.900	4.06×10^{-6}	9427	10.403	2.310	0.7582	75.82

Note: E_{corr}: Corrosion potential; I_{corr}: Corrosion current density; R_p: Polarization resistance; β_a: anodic current; β_c: cathodic current; θ: surface coverage; IE: Inhibition efficiency.

Figure 8 represents *Coriandrum sativum* that effectively inhibited the rate of microbe-induced corrosion. In the case of *Coriandrum sativum*–mediated inhibition of biocorrosion, the order of inhibition is as follows: *Klebsiella pneumonia* > *Staphylococcus aureus* = *Bacillus subtilis*. The E_{corr} value shows that microbial corrosion by *Staphylococcus aureus* and *Bacillus subtilis* was effectively

inhibited by the plant extract, but the polarization curve of *Klebsiella pneumonia* was more negative compared to CTW + *Klebsiella pneumonia* + plant extract. A high negative value warranted a higher corrosion rate based on the E_{corr} value. Moreover, the I_{corr} value of *Klebsiella pneumonia* is high compared to *Staphylococcus aureus* and *Bacillus subtilis*. Polarization resistance (R_p) of the investigation in all the categories demonstrated that plant extract–mediated microbial corrosion was found to be low in most of the categories, while some extracts were not able to inhibit the corrosion due to high polarization resistance.

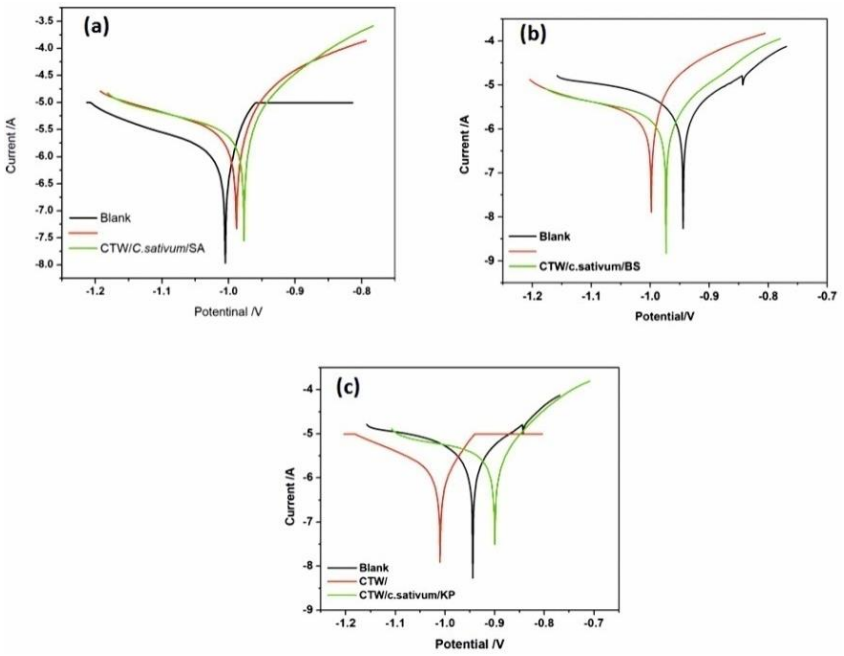

Figure 8. Corrosion and biocorrosion mediated by *Coriandrum sativum*.

3.6. Weight loss

Weight loss, corrosion, and metal instability are all influenced by the solubility of metal in the solution. When inhibitors are added, the weight loss of the specimens reduces linearly with the corrosion rate [53] The extract contains phyto-constituents with anti-microbial action, which prevents microbes from adhering to and harboring on the metal's exterior. This reduces the formation of biofilms and biocorrosion [54].

In the case of *Bacillus subtilis* and *Klebsiella pneumonia*, the weight loss was reported to be 0.018 and 0.011 g, with a corrosion rate of 3.83 and 2.47 mm/year respectively. The results indicate that *Bacillus subtilis* induced more corrosion with maximum weight loss. The corrosion inhibition efficiencies were found to be 83.6%, 78.5%, and 86.6% for the respective systems after 21 days. After 21 days of exposure, weight loss was 0.017, 0.018, and 0.0174 g, and corrosion rates were 3.7, 4.0, and 3.71 mm/year, for *S. aureus, B. subtilis, and K. pneumonia*, respectively. Various factors such as phyto-constituents, extract concentration, extraction solvent, extraction temperature, mild steel coupon exposure duration, and operating temperature have been reported to play a vital role in varying the corrosion inhibition efficiencies of plant extracts [36]. From the weight loss experiments,

it was concluded that at an optimum plant extract concentration of 30 ppm, the biocorrosion of mild steel was inhibited by more than 70%.

4. Conclusions

This study looked into the effectiveness of three plant extracts as microbial corrosion inhibitors for mild steel coupons. To determine the lowest inhibitory concentration, the well diffusion method was employed. The ideal dosage for biocorrosion inhibition on mild steel coupons was found to be 30 ppm, as this produced a distinct zone of inhibition. Following three weeks, the weight loss approach demonstrated over 70% corrosion inhibition efficiency against *S. aureus*, *B. subtilis*, and *K. pneumoniae* by the inhibitor systems containing *C. sativum*.

Polarization investigations showed that while the Rp values were higher than those of the control and microbial systems, I_{corr} decreased in the presence of plant inhibitors. The I_{corr} value in the control system was 1.68×10^{-5} A/cm^2, and the microbial system had a somewhat higher I_{corr}. The development of biofilm and the growth of microorganisms may be the cause of the increased corrosion current in the microbial system. Nonetheless, it was discovered that Icorr was lower in the presence of the green inhibitors than in the microbial and control systems. Rp exceeded that of the microbiological and control systems when the inhibitors were present. Thus, once the plant inhibitors were added, the corrosion current density decreased, and the Rp values increased. The Ecorr graph displayed anodic inhibitor behavior, since the inhibitor system's maximum displacement was 1.0 V or 1000 mV, which was higher than 85 mV. *C. sativum* led to 81.00%, 84.38%, and 75.62% of inhibitory efficiency against *S. aureus*, *B. subtilis*, and *K. pneumoniae*, respectively.

According to the impedance experiments, there was a drop in C_{dl} values and an increase in Rs and R_{ct} values in relation to the plant inhibitors. The findings from the mild steel Nyquist plot curves showed that the inhibitor system had greater R_s and R_{ct} values than the microbial system. *C. sativum* was responsible for 87.95%, 93.05%, and 87.51% of inhibitory efficiency against *S. aureus*, *B. subtilis*, and *K. pneumoniae*, respectively. SEM pictures demonstrated uniform corrosion and moderate biofilm formation in the control system, thick biofilm formation in the microbial system, and little biofilm formation in the inhibitor system. Biocorrosion was prevented in the inhibitor system by the potential functional groups of the extract's active ingredients, which were determined by the peak bands in the FT-IR spectra. The inhibitors utilized in this study have functional groups connected to the metal, which acted as a protective layer and were the primary cause of the biofilm's suppression, according to the GC–MS spectra. By using GC–MS analysis, the adsorption of active ingredients like linalool in *C. sativum* was verified.

In this work, weight loss studies, electrochemical studies, XRD, SEM, FT-IR, and GC–MS analysis data clarified the microbes responsible for mild steel corrosion. However, these may be inhibited by green inhibitors when these are used at the optimal dosage of 30 ppm plant extract in cooling tower water. The plant extract's phytoactive components were responsible for inhibiting mild steel's biocorrosion. The plant extracts' functional groups inhibited the formation of biofilms by adsorbing themselves on the mild steel.

Use of Generative-AI tools declaration

The author(s) declare(s) they have used Artificial Intelligence (AI) tools in the creation of this article.

Author contributions

Sharmil Suganya R: Planning and conduction of experiments, result analysis and manuscript writing; Stanelybritto Maria Arul Francis: Conduction of experiments and result analysis; Venugopal T: Editing the manuscript and manuscript writing.

Acknowledgments

We are quite grateful to the Government College of Engineering, Salem, for funding and providing facilities for the study and providing us with the opportunity to successfully finish our research project. We would like to express our gratitude to the Department of Chemistry Laboratory's scientific team for their important support during the experimental investigation.

Conflict of interest

The authors declare that there is no conflict of interest.

References

1. Hamak KF (2014) Synthesis of phthalimides via the reaction of phthalic anhydride with amines & evaluating of its biological & anti-corrosion activity. *Int J Chem Tech Res* 6: 324–333.
2. El-Shanshoury AER, ElSilk S, Ebeid ME (2011) Extracellular biosynthesis of silver nanoparticles using *Escherichia coli* ATCC 8739, *Bacillus subtilis* ATCC 6633, and *Streptococcus thermophilus* ESh1 and their antimicrobial activities. *Int Scholarly Res Notices* 2011: 385480. https://doi.org/10.5402/2011/385480
3. Sahib NG, Anwar F, Gilani AH, et al. (2012) Coriander (*Coriandrum sativum* L.): A potential source of high-value components for functional foods and nutraceuticals-A review. *Phytother Res* 27: 1439–1456. https://doi.org/10.1002/ptr.4897
4. Kubo I, Fujita KI, Kubo A, et al. (2004) Antibacterial activity of coriander volatile compounds against *Salmonella cholerasuis*. *J Agric Food Chem* 52: 3329–3332. https://doi.org/10.1021/jf0354186
5. Saeed S, Tariq P (2007) Antimicrobial activities of *Emblica officinalis* and *Coriandrum sativum* against Gram-positive bacteria and *Candida albicans*. *Pak J Bot* 39: 913–917.
6. Begnami AF, Duarte MCT, Furletti V, et al. (2010) Antimicrobial potential of *Coriandrum sativum* L. against different *Candida* species *in vitro*. *Food Chem* 118: 74–77. https://doi.org/10.1016/j.foodchem.2009.04.089
7. Al-Snafi AE (2016) A review on chemical constituents and pharmacological activities of *Coriandrum sativum*. *IOSR J Pharm* 6: 17–42. https://doi.org/10.9790/3013-067031742

8. Sastri BN (1950) *Coriandrum sativum* Linn (Umbelliferae). In: *The wealth of India: A dictionary of Indian raw materials and industrial products (Vol 2)*. New Delhi: Council of Scientific and Industrial Research, 347–350.
9. WFO (2024) Coriandrum sativum L. Available from: http://www.worldfloraonline.org/tpl/kew-2737546.
10. Da Rocha Magalhães L, da Silva Alvarenga RF, Resende FAC, et al. (2023) The synergy between corrosion and fatigue: Failure analysis of an aerator and a cooling tower. *J Fail Anal Prev* 23: 1803–1819. https://doi.org/10.1007/s11668-023-01729-1
11. Kokilaramani S, Al-Ansari MM, Rajasekar A, et al. (2021) Microbial influenced corrosion of processing industry by re-circulating wastewater and its control measures—A review. *Chemosphere* 265: 129075. https://doi.org/10.1016/j.chemosphere.2020.129075
12. Telegdi J, Shaban A, Trif L (2017) Microbiologically influenced corrosion (MIC). In: *Trends in oil and gas corrosion research and technologies*. 191–214. https://doi.org/10.1016/B978-0-08-101105-8.00008-5
13. Kuraimid ZK, Majeed HM, Jebur HQ, et al. (2021) Synthesis of new corrosion inhibitors with high efficiency in aqueous and oil phase for low carbon steel for Missan oil field equipment. *Eurasian Chem Commun* 3: 860–871. https://doi.org/10.22034/ecc.2021.302887.1233
14. Kaya F, Solmaz R, Gecibesler IH (2023) Adsorption and corrosion inhibition capability of*Rheum ribes*root extract (*Işgın*) for mild steel protection in acidic medium: A comprehensive electrochemical, surface characterization, synergistic inhibition effect, and stability study. *J Mol Liq* 372: 121219. https://doi.org/10.1016/j.molliq.2023.121219
15. Hossain SMZ, Razzak SA, Hossain MM (2020) Application of essential oils as green corrosion inhibitors. *Arab J Sci Eng* 45: 7137–7159. https://doi.org/10.1007/s13369-019-04305-8
16. Sezonov G, Joseleau-Petit D, D'Ari R (2007) *Escherichia coli* physiology in Luria-Bertani broth. *J Bacteriol* 189: 8746–8749. https://doi.org/10.1128/JB.01368-07
17. Balouiri M, Sadiki M, Ibnsouda SK (2016) Methods for *in vitro* evaluating antimicrobial activity: A review. *J Pharm Anal* 6: 71–79. https://doi.org/10.1016/j.jpha.2015.11.005
18. Narenkumar J, Parthipan P, Nanthini AUR, et al. (2017) Ginger extract as green biocide to control microbial corrosion of mild steel. *3 Biotech* 7: 133. https://doi.org/10.1007/s13205-017-0783-9
19. Rajasekar V, Shyamala M, Aravind J (2024) Green, environmentally friendly synthesis of MnO nanoparticles for corrosion inhibition in mild steel, *Glob NEST J* 26: 1–12. https://doi.org/10.30955/gnj.05891
20. Nwigwe US, Mbam SO, Umunakwe R (2019) Evaluation of *Carica papaya* leaf extract as a bio-corrosion inhibitor for mild steel applications in a marine environment. *Mater Res Express* 6: 105107. https://doi.org/10.1088/2053-1591/ab3ff6
21. Agarry SE, Oghenejoboh KM, Aworanti OA, et al. (2019) Biocorrosion inhibition of mild steel in crude oil-water environment using extracts of *Musa paradisiaca* peels, *Moringa oleifera* leaves, and *Carica papaya* peels as biocidal-green inhibitors: Kinetics and adsorption studies. *Chem Eng Commun* 206: 98–124. https://doi.org/10.1080/00986445.2018.1476855
22. Karunanithi A, Venkatachalam S (2019) Ultrasonic-assisted solvent extraction of phenolic compounds from *Opuntia ficus-indica* peel: Phytochemical identification and comparison with Soxhlet extraction. *J Food Process Eng* 42: e13126. https://doi.org/10.1111/jfpe.13126

23. Pal MK, Lavanya M (2022) Microbial influenced corrosion: Understanding bioadhesion and biofilm formation. *J Bio TriboCorros*8: 76.https://doi.org/10.1007/s40735-022-00677-x
24. Loto CA (2017) Microbiological corrosion: Mechanism, control, and impact—A review. *Int J Adv Manuf Technol* 92: 4241–4252.https://doi.org/10.1007/s00170-017-0494-8
25. Knisz J, Eckert R, Gieg LM, et al. (2023) Microbiologically influenced corrosion—more than just microorganisms. *FEMS Microbiol Rev* 47: fuad041. https://doi.org/10.1093/femsre/fuad041
26. Molina RDI, Campos-Silva R, Macedo AJ, et al. (2020) Antibiofilm activity of coriander (*Coriander sativum* L.) grown in Argentina against food contaminants and human pathogenic bacteria. *Ind Crops Prod* 151: 112380. https://doi.org/10.1016/j.indcrop.2020.112380
27. Lin Q, Li Y, Sheng M, et al. (2023) Antibiofilm effects of berberine-loaded chitosan nanoparticles against *Candida albicans* biofilm. *LWT* 173: 114237. https://doi.org/10.1016/j.lwt.2022.114237
28. da Silva BD, Bernardes PC, Pinheiro PF, et al. (2021) Chemical composition, extraction sources, and action mechanisms of essential oils: Natural preservative and limitations of use in meat products. *Meat Sci* 176: 108463. https://doi.org/10.1016/j.meatsci.2021.108463
29. Caldwell DE, Korber DR, Lawrence LR (1992) Confocal laser microscopy and digital image analysis in microbial ecology. In: *Advances in microbial ecology*. Boston, MA: Springer, 1–67. https://doi.org/10.1007/978-1-4684-7609-5_1
30. Mohd Ali MKFB, Abu Bakar A, Noor NM, et al. (2017) Hybrid soliwave technique for mitigating sulfate-reducing bacteria in controlling biocorrosion: A case study on crude oil sample. *Environ Technol* 38: 2427–2439. https://doi.org/10.1080/09593330.2016.1264486
31. Albahri MB, Barifcani A, Iglauer S, et al. (2021) Investigating the mechanism of microbiologically influenced corrosion of carbon steel using X-ray micro-computed tomography. *J Mater Sci* 56: 13337–13371. https://doi.org/10.1007/s10853-021-06112-9
32. Malek TJ, Chaki SH, Deshpande MP (2018) Structural, morphological, optical, thermal and magnetic study of mackinawite FeS nanoparticles synthesized by wet chemical reduction technique. *Physica B* 546: 59–66. https://doi.org/10.1016/j.physb.2018.07.024
33. Otton LM, da Silva Campos M, Meneghetti KL, et al. (2017) Influence of twitching and swarming motilities on biofilm formation in *Pseudomonas* strains. *Arch Microbiol* 199: 677–682. https://doi.org/10.1007/s00203-017-1344-7
34. Karthik R, Muthukrishnan P, Chen SM, et al. (2015) Anti-corrosion inhibition of mild steel in 1M hydrochloric acid solution by using *Tiliacora accuminata* leaves extract. *Int J Electrochem Sci* 10: 3707–3725.https://doi.org/10.1016/S1452-3981(23)06573-2
35. AlSalhi MS, Devanesan S, Rajasekar A, et al. (2023) Characterization of plants and seaweeds based corrosion inhibitors against microbially influenced corrosion in a cooling tower water environment. *Arab J Chem* 16: 104513. https://doi.org/10.1016/j.arabjc.2022.104513
36. Sourmaghi MH, Kiaee G, Golfakhrabadi F, et al. (2015) Comparison of essential oil composition and antimicrobial activity of *Coriandrum sativum* L. extracted by hydrodistillation and microwave-assisted hydrodistillation. *J Food Sci Technol* 52: 2452–2457. https://doi.org/10.1007/s13197-014-1286-x
37. Murungi PI, Sulaimon AA (2022) Ideal corrosion inhibitors: A review of plant extracts as corrosion inhibitors for metal surfaces. *Corros Rev* 40: 127–136. https://doi.org/10.1515/corrrev-2021-0051

38. Videla HA (1996) *Manual of biocorrosion*. New York: Routledge. https://doi.org/10.1201/9780203748190
39. Ech-chihbi E, Adardour M, Ettahiri W, et al. (2023) Surface interactions and improved corrosion resistance of mild steel by addition of new triazolyl-benzimidazolone derivatives in acidic environment. *J Mol Liq* 387: 122652. https://doi.org/10.1016/j.molliq.2023.122652
40. Cai T, Zhang Y, Wang N, et al. (2022) Electrochemically active microorganisms sense charge transfer resistance for regulating biofilm electroactivity, spatio-temporal distribution, and catabolic pathway. *Chem Eng J* 442: 136248. https://doi.org/10.1016/j.cej.2022.136248
41. Pais M, Rao P (2021) Electrochemical, spectroscopic and theoretical studies for acid corrosion of zinc using glycogen. *Chem Pap*75: 1387–1399. https://doi.org/10.1007/s11696-020-01391-z
42. Xu D, Li Y, Gu T (2016) Mechanistic modelling of biocorrosion caused by biofilms of sulfate reducing bacteria and acid producing bacteria. *Bioelectrochemistry* 110: 52–58. https://doi.org/10.1016/j.bioelechem.2016.03.003
43. Karn SK, Fang G, Duan J (2017) *Bacillus sp.* acting as dual role for corrosion induction and corrosion inhibition with carbon steel (CS). *Front Microbiol* 8: 02038. https://doi.org/10.3389/fmicb.2017.02038
44. Farh HMH, Ben Seghier MEA, Zayed T (2023) A comprehensive review of corrosion protection and control techniques for metallic pipelines. *Eng Fail Anal* 143: 106885. https://doi.org/10.1016/j.engfailanal.2022.106885
45. Kumari PP, Shetty P, Rao SA (2017) Electrochemical measurements for the corrosion inhibition of mild steel in 1M hydrochloric acid by using an aromatic hydrazide derivative. *Arab J Chem* 10: 653–663. https://doi.org/10.1016/j.arabjc.2014.09.005
46. Narenkumar J, Parthipan P, Madhavan J, et al. (2018) Bioengineered silver nanoparticles as potent anti-corrosive inhibitor for mild steel in cooling towers. *Environ Sci Pollut Res* 25: 5412–5420. https://doi.org/10.1007/s11356-017-0768-6
47. Permeh S, Lau K, Duncan M (2019) Characterization of biofilm formation and coating degradation by electrochemical impedance spectroscopy. *Coatings* 9: 518. https://doi.org/10.3390/coatings9080518
48. Fojt J, Průchová E, Hybášek V (2023) Electrochemical impedance response of the nanostructured Ti–6Al–4V surface in the presence of *S. aureus* and *E. coli*. *J Appl Electrochem* 53: 2153–2167. https://doi.org/10.1007/s10800-023-01911-1
49. Kim T, Kang J, Lee JH, et al. (2011) Influence of attached bacteria and biofilm on double-layer capacitance during biofilm monitoring by electrochemical impedance spectroscopy. *Water Res* 45: 4615–4622. https://doi.org/10.1016/j.watres.2011.06.010
50. Victoria SN, Sharma A, Manivannan R (2021) Metal corrosion induced by microbial activity–Mechanism and control options. *J Indian Chem Soc* 98: 100083. https://doi.org/10.1016/j.jics.2021.100083
51. Caldona EB, de Leon ACC, Mangadlao JD, et al. (2018) On the enhanced corrosion resistance of elastomer-modified polybenzoxazine/graphene oxide nanocomposite coatings. *React Funct Polym* 123: 10–19. https://doi.org/10.1016/j.reactfunctpolym.2017.12.004
52. Olasunkanmi LO, Obot IB, Kabanda MM, et al. (2015) Some quinoxalin-6-yl derivatives as corrosion inhibitors for mild steel in hydrochloric acid: Experimental and theoretical studies. *J Phys Chem C* 119: 16004–16019. https://doi.org/10.1021/acs.jpcc.5b03285

53. Rao P, Mulky L (2023) Microbially influenced corrosion and its control measures: A critical review. *J Bio Tribo Corros* 9: 57. https://doi.org/10.1007/s40735-023-00772-7
54. Briggs WF, Stanley HO, Okpokwasili GC, et al. (2019) Biocorrosion inhibitory potential of aqueous extract of *Phyllanthus amarus* against acid-producing bacteria. *J Adv Biol Biotechnol* 22: 1–8. https://doi.org/10.9734/jabb/2019/v22i130106

AIMS Press